



tonian in [7]:

$$\begin{aligned}\mathcal{H}(t) &= \mathcal{H}_0 + \mathcal{H}'(t) \\ \mathcal{H}_0 &= \mathcal{H}_L + \mathcal{H}_B + \mathcal{H}_R\end{aligned}\quad (1)$$

$$\mathcal{H}'(t) = \alpha_L(t)\mathcal{V}_L + \alpha_R(t)\mathcal{V}_R \quad (2)$$

The specific choice of various parts of the Hamiltonian is as follows. The three parts of the structure, taken as separate, have no time dependence. The leads, labeled by  $L$  and  $R$ , couple only to the bridge  $B$ , but not one to another. The coupling is specified by time independent operator amplitudes  $\mathcal{V}_{L,R}$  coupling the leads to the central island orbital. All time dependence in the model is concentrated into two scalar functions  $\alpha_{L,R}(t)$ . These functions may be arbitrary, but to describe the switching processes, we will assume them to jump suddenly between 0 and 1, describing a disconnected and connected junction respectively. With the use of an adiabatic process starting from  $\mathcal{H}_0$  at  $t = -\infty$ , it is easy to obtain the Keldysh NGF [8] for the central island orbital. We employ the Langreth-Wilkins convention[10] and construct the triplet of propagators  $G^R, G^A$  and the "less" particle correlation function  $G^<$  of Kadanoff and Baym [9]. The Dyson equations for the propagators have the form

$$G^{R,A} = G_0^{R,A} + G_0^{R,A} \Sigma^{R,A} G^{R,A}, \text{ etc.} \quad (3)$$

while the less component satisfies the Dyson equation

$$G^< = G^R \Sigma^< G^A \quad (4)$$

All components of the self-energy have the form

$$\begin{aligned}\Sigma^X(t, t') &= \Sigma_L^X(t, t') + \Sigma_R^X(t, t') \\ \Sigma_Y^X(t, t') &= \alpha_Y(t) \sigma_Y^X(\tau) \alpha_Y(t') \\ \sigma_Y^{R,A}(\tau) &= \pm i \int \frac{dE}{2\pi} \Delta_Y(E) e^{-iE\tau} \vartheta(\pm\tau) \\ \sigma_Y^<(\tau) &= i \int \frac{dE}{2\pi} \Delta_Y(E) f_Y(E) e^{-iE\tau} \\ \tau &= t - t', \quad X = R, A, < \quad Y = L, R\end{aligned}\quad (5)$$

Each fully connected junction is thus associated with a spectral function  $\Delta_Y$  which, together with the quasi-equilibrium Fermi function  $f_Y$ , specifies the  $Y$  self-energy triplet. Customarily, the spectral function is taken as flat (so-called wide band limit). In fact, this function is physically very similar to the adsorption function of Grimley or Newns [11] and may have a pronounced spectral structure which is transferred into the short time behavior of the self-energy[5].

In principle, any time-dependent process at the bridge is now solved. It is both productive and illuminating to make one more step, however, and view a transient starting at a finite time  $t_1$  as embedded into the complete Keldysh "host" process[5]. This does not affect the propagators, but the Dyson

equation for the restricted less function is now more involved [12, 13]:

$$\begin{aligned}G_1^< &= G^R \Sigma_1^< G^A, \\ \Sigma_1^< &= \overset{\circ}{\Sigma}_1^< + \overset{\bullet}{\Sigma}_1^< + \overset{\circ}{\Sigma}_1^{\circ} + \overset{\bullet}{\Sigma}_1^{\circ}\end{aligned}\quad (6)$$

Here,  $\Sigma_1^<$  denotes the complete less self-energy of the transient, the symbolic multiplications involve integrations starting at  $t_1$ . The self-energy is modified so as to compensate for this restricted integration area. The four components of  $\Sigma_1^<$  differ by the behavior at  $t_1$ , as indicated by circles.  $\circ \dots$  time variable fixed at  $t_1$ ,  $\bullet \dots$  time variable continuous in  $(t_1, \infty)$ . Thus[5],

$$\begin{aligned}\overset{\circ}{\Sigma}_1^<(t, t') &= i\rho_1(t_1)\delta(t-t_1-0)\delta(t'-t_1-0), \\ \overset{\bullet}{\Sigma}_1^<(t, t') &= \overset{\circ}{\Lambda}_1^<(t_1, t')\delta(t-t_1-0), \\ \overset{\circ}{\Sigma}_1^{\circ}(t, t') &= \overset{\circ}{\Lambda}_1^{\circ}(t, t_1)\delta(t'-t_1-0) \\ \overset{\bullet}{\Sigma}_1^{\circ}(t, t') &= \Sigma^<(t, t') + \overset{\circ}{\Sigma}_1^<(t, t')\end{aligned}\quad (7)$$

The initial occupation  $\rho(t_1)$  of the island orbital in the first line, and the host self-energy  $\Sigma^<$  in the fourth line would describe the transient, if the initial state was an equilibrium state of the unperturbed Hamiltonian  $\mathcal{H}_0$  ( $\dots$  a one-particle analogue of an uncorrelated initial condition). The additional quantities  $\overset{\circ}{\Lambda}_1^<$ ,  $\overset{\circ}{\Lambda}_1^{\circ}$  and  $\overset{\circ}{\Sigma}_1^<$  describe the initial correlation, or, put alternatively, the influence of past evolution on the commencing transient. We have developed a method of partitioning-in-time to construct these correction terms from the known NGF of the host process [14].

In the present case, the partitioning procedure can be extended into an iterative procedure. Let

$$-\infty \equiv t_0 \ll t_1 < t_2 \dots < t_n < t_{n+1} \dots \quad (8)$$

be the sequence of switching times with quiescent time intervals in between. We choose the  $t_n$  instants as the starting times of transient processes, the  $n+1$ th process embedded in the  $n$ th one. Then  $G_{n+1}^<(t, t')$  for  $t, t' > t_{n+1}$ , and with lower integration limit  $t_{n+1}$ , becomes

$$\begin{aligned}G_{n+1}^< &= G^R \Sigma_{n+1}^< G^A, \\ \Sigma_{n+1}^< &= \overset{\circ}{\Sigma}_{n+1}^< + \overset{\bullet}{\Sigma}_{n+1}^< + \overset{\circ}{\Sigma}_{n+1}^{\circ} + \overset{\bullet}{\Sigma}_{n+1}^{\circ}\end{aligned}\quad (9)$$

The self-energy is constructed from  $G_n^<(t, t')$  known for  $t, t' > t_n$ . To avoid clumsy expressions, we illustrate the procedure by one example,

$$\begin{aligned}\overset{\circ}{\Lambda}_{n+1}^<(t_{n+1}, u) &= i \int_{t_n}^{t_{n+1}} d\bar{t} \{ G^R \Sigma_n^< + G_n^< \Sigma^A \} \\ G^R \Sigma_n^< &\mapsto G^R(t_{n+1}, \bar{t}) \Sigma_n^<(\bar{t}, u), \text{ etc.}\end{aligned}\quad (10)$$

Using (5), (8) and prescribing the switching sequence, these expressions can be made much more explicit. Presently more important is to observe that actual integration limits in Eq. (10)

may be narrowed[14]: the function  $\Sigma_n^<(t, t')$  is nearly zero for  $|t - t'| > \tau_c$ , a characteristic decay time of correlations. The integration in (10) and all related expressions will thus extend from  $\max(t_n, t_{n+1} - \tau_c)$  to  $t_{n+1}$ . The resulting transient behavior will depend on the degree of overlap of the subsequent processes of correlation decay, as indicated by the relative position of  $t_n + \tau_c$  and  $t_{n+1} - \tau_c$ .

### 3 Response to switching junctions on and off

For actual calculations, the metallic leads were taken as identical. The spectral function  $\Delta_y(E)$  was broad, but with a resonant structure (FWHM 0.3 eV). This, together with the step-like distribution function  $f_y(E)$  gave rise to  $\tau_c \approx e$  in the 10 fs range. The assumed sudden switching events, may thus simulate processes with femtosecond switching times. The leads had constant bias  $\pm 0.5\text{eV}$  with respect to the island level, so that the charge flowed from the  $L$  lead to the  $R$  one on the whole. At the initial time  $t_1 = 0$  of the transient, the level was empty and disconnected from both leads. For  $t > t_1$ , the currents through both junctions were calculated from the usual formulas [7], or their partitioning derivatives.

#### 3.1 Case A: Island suddenly connected to the leads

As the first **Case A**, we show the transient induced by switching both junctions on at  $t_1 = 0$  (studied in the wide band limit in [4]). Fig. 1 shows initial oscillations of the currents  $J_L, J_R$  at both junctions, followed after elapsing about 20 fs by balanced steady currents. Correspondingly the rate of occupancy of the island level first oscillates and saturates to zero. A deeper insight is provided by Fig. 2 showing  $G^<$  as a double time function. The crest line of the plot along the diagonal  $t = t'$  is the occupation number  $\rho(t) = iG^<(t, t)$ . It exhibits three stages: initial oscillatory transient, gradual saturation at controlled by the transport relaxation time and finally the steady state.

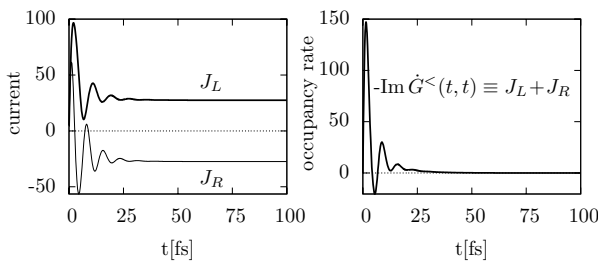


**Fig. 1 Case A.** Left panel: junction currents. Right panel: current balance at the island

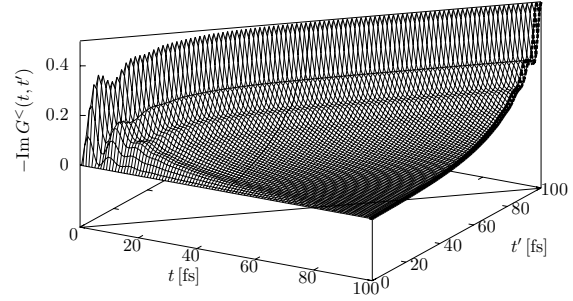


**Fig. 2 Case A.** Particle correlation function  $G^<$ . Darker part: steady state

#### 3.2 Multiple switching

The next simplest **Case B** is specified by the sequence of switching events:  $t_1 = 0$  fs :  $L$  on,  $t_2 = 40$  fs :  $R$  on,  $t_3 = 70$  fs :  $R$  off,  $t_4 = 80$  fs :  $R$  on. The  $L$  junction remains connected, while the  $R$  junction undergoes the switching on and off alternately.

In Figs. 3, 4, 5, the currents are shown for three subcases **B1**, **B2**, **B3**, whose label indicates the number of switch overs undergone by the  $R$  junction. As before, each switching induces first the transitory current oscillations, which die out gradually. The sign of the initial oscillation is such that the  $R$  junction "overreacts" at first and this is compensated later by the continued transient. It should be noted that the  $L$  junction invariably responds to the state of the  $R$  junction. Because the two junctions act differently having a mutually opposite bias, the  $L$  junction contributes to the compensation of the initial transient at the  $R$  junction. This is neatly demonstrated at the total occupancy rates. See Fig. 3 for **B1**. Turning the  $R$  junction off, Fig. 4 for **B2**, causes a transient reaction at  $L$ . The  $J_L$  current continues to flow by inertia at first and slows down in a wavy manner. Finally, in Fig. 5 for **B3**, we see how the next switch on coming early interrupts this process and the system returns to the final state of **B1**, but in an irregular manner caused by the overlap and mutual coupling of the two last transients.

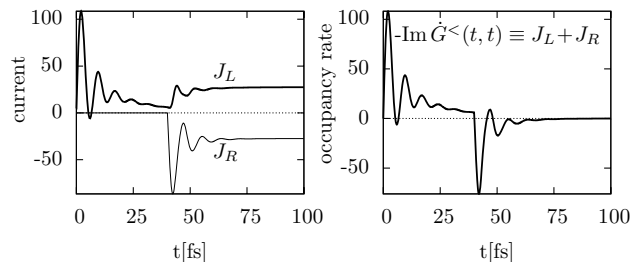


**Fig. 3 Case B1** – see text. Left panel: junction currents. Right panel: current balance at the island

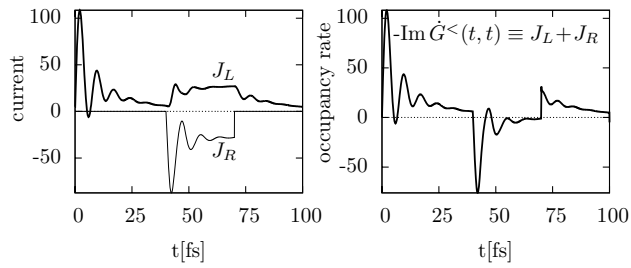


**Fig. 4 Case B2** – see text. Left panel: junction currents. Right panel: current balance at the island

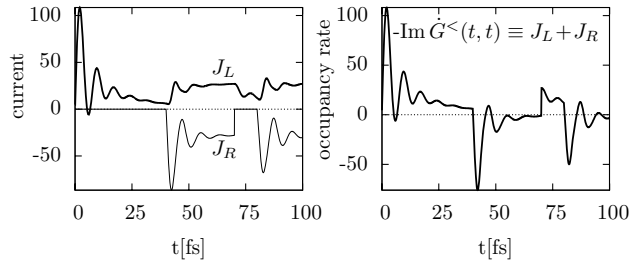


**Fig. 5 Case B3** – see text. Left panel: junction currents. Right panel: current balance at the island

The richest **B3** process is further illuminated by Fig. 6 which displays the imaginary part of  $G^<$  and can be compared with Fig. 2. The crest line represents the response of the island level occupation to the whole sequence of  $R$  switch-overs. The slopes of the whole plot (the symmetric one is hidden from the view) indicate the range of the coherent coupling of different areas. Clearly visible are the imprints of the  $t = t_n$  and the  $t' = t_n$  lines and the penetration of the coherent oscillations across these discontinuities.

It has been pointed out in Sec. 2 that the time partitioning permits to distinguish the correlated initial conditions from the uncorrelated ones by the presence of corrections to the less self-energy. This is demonstrated by Fig. 7 which shows one of the corrections,  $\widehat{\Sigma}_n^<$ . (see the last line of Eq. (7)). There is no correction at the leftmost corner  $t = t' = t_1$ , because there is no coherence between the past of the disconnected junction and the ensuing transient. By contrast, all later switch-overs give rise to a reconstruction of the initial state of the system and the correlation correction emerge. They die out soon, so that only the last pair,  $t_2$  and  $t_3$ , appears to have the correlation correction overlapping and thus coupled.

## References

1. M. Galperin, M. A. Ratner, and A. Nitzan, Molecular transport junctions: vibrational effects, *J. Phys.: Cond. Matt.* **19**, 103201 (2007).
2. G. Stefanucci, Bound states in ab initio approaches to quantum transport: A time-dependent formulation, *Phys. Rev. B* **75**, 195115 (2007).

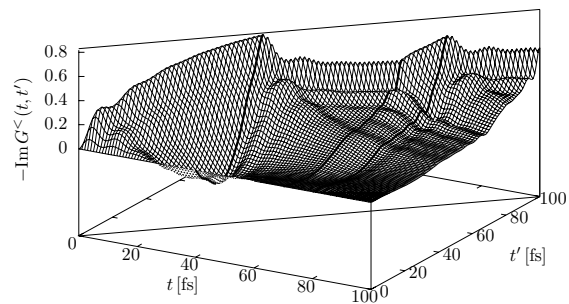


**Fig. 6 Case B3.** Particle correlation function  $G^<$ . See text

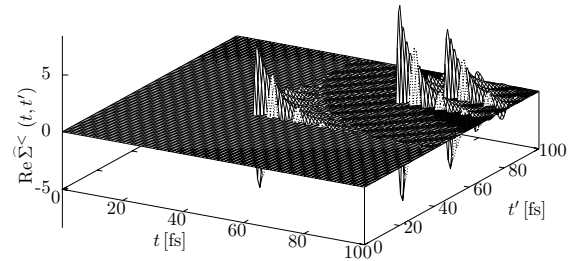


**Fig. 7 Case B3.** Correlation corrections  $\widehat{\Sigma}_n^<$  to the lesser self-energy.

3. D.F. Urban, R. Avriiler, and A. Levy Yeyati, Nonlinear effects of phonon fluctuations on transport through nanoscale junctions, *Phys. Rev. B* **82**, 121414(R) (2010).
4. T.L. Schmidt, P. Werner, L. Muhlbacher, and A. Komnik, Transient dynamics of the Anderson impurity model out of equilibrium, *Phys. Rev. B* **78**, 235110 (2008).
5. B. Velický, A. Kalvová and V. Špička, Single molecule bridge as a testing ground for using NGF outside of the steady current regime, *Physica E* **42**, 539 (2010).
6. Y. Meir, N.S. Wingreen, Landauer formula for the current through an interacting electron region, *Phys. Rev. Lett.* **68**, 2512 (1992).
7. A. P. Jauho, N.S. Wingreen and Y. Meir, Time-dependent transport in interacting and noninteracting resonant tunneling systems, *Phys. Rev. B* **50**, 5528 (1994).
8. L.V. Keldysh, Diagram technique for nonequilibrium processes, *Sov. Phys. JETP* **20**, 1018 (1965).
9. L. P. Kadanoff and G. Baym, *Quantum Statistical Mechanics*, (Benjamin, New York, 1962).
10. D. C. Langreth and G. Wilkins, Theory of spin resonance in dilute magnetic alloys, *Phys. Rev. B* **6**, 3189 (1972).
11. D.M. News, Self-consistent model of hydrogen chemisorption, *Phys. Rev.* **178**, 1123 (1969), T.B. Grimley, Electronic structure of adsorbed atoms and molecules, *J. Vac. Sci. Technol.* **8**, 31 (1971).
12. P. Danielewicz, Quantum theory of nonequilibrium processes, *Ann. Phys. (N.Y.)* **152**, 239 (1984).
13. M. Wagner, Expansion of nonequilibrium Green's functions, *Phys. Rev. B* **44**, 6104 (1991).
14. B. Velický, A. Kalvová and V. Špička, Correlated initial condition for an embedded process by time partitioning, *Phys. Rev. B* **81**, 235116 (2010).